Available online at www.sciencedirect.com

ScienceDirect

journal homepage: www.intl.elsevierhealth.com/journals/dema

Aging resistant ZTA composite for dental applications: Microstructural, optical and mechanical characterization

Ernesto Byron Benalcazar Jalkh[a,f,*], *Kelli Nunes Monteiro*[b], *Paulo Francisco Cesar*[b], *Luis Antonio Genova*[c], *Edmara T.P. Bergamo*[a], *Adolfo Coelho de Oliveira Lopes*[a], *Erick Lima*[b], *Paulo Noronha Lisboa-Filho*[d], *Tiago Moreira Bastos Campos*[e], *Lukasz Witek*[f,g], *Paulo G. Coelho*[f,h,i], *Ana Flavia Sanches Borges*[j], *Estevam A. Bonfante*[a]

[a] *Department of Prosthodontics and Periodontology, University of São Paulo, Bauru School of Dentistry, Bauru, SP, Brazil*
[b] *Department of Biomaterials and Oral Biology, University of São Paulo, School of Dentistry, SP, Brazil*
[c] *Institute of Research in Nuclear Energy, SP, Brazil*
[d] *Department of Physics, São Paulo State University, Bauru, SP, Brazil*
[e] *Technological Institute of Aeronautics, São José dos Campos, SP, Brazil*
[f] *Department of Biomaterials and Biomimetics, New York University College of Dentistry, New York, NY, USA*
[g] *Department of Biomedical Engineering, New York University, Tandon School of Engineering, Brooklyn, NY, USA*
[h] *Hansjörg Wyss Department of Plastic Surgery, NYU Langone Medical Center, New York, NY, USA*
[i] *Mechanical and Aerospace Engineering, NYU Tandon School of Engineering, New York, NY, USA*
[j] *Department of Operative Dentistry, Endodontics and Dental Materials, University of São Paulo - Bauru School of Dentistry, Bauru, SP, Brazil*

ARTICLE INFO

Article history:
Received 9 November 2019
Received in revised form 3 May 2020
Accepted 24 May 2020

Keywords:
Composites
ZrO_2–Al_2O_3
Mechanical properties
Optical properties
Microstructure

ABSTRACT

Objective. To synthesize a zirconia toughened alumina (ZTA) composite with 70% alumina reinforced by 30% zirconia for dental applications and to characterize its microstructure and optical properties for comparison with the isolated counterpart materials and a first-generation 3Y-TZP.

Methods. Disc-shaped specimens were divided in four groups (n = 70/material): (1) 3YSB-E (first generation 3Y-TZP), (2) Zpex (second generation 3Y-TZP), (3) alumina, and (4) ZTA-Zpex 70/30. After synthesis, ceramic powders were pressed, and green-body samples sintered following a predetermined protocol. Specimens were polished to obtain a mirror surface finish. Apparent density was measured by Archimedes principle. X-ray diffraction (XRD) and scanning electron microscope (SEM) were used to characterize the crystalline content and microstructure. Reflectance tests were performed to determine the contrast-ratio (CR) and translucency-parameter (TP). Mechanical properties were assessed by biaxial flexural strength (BFS) test. All analyses were conducted before and after artificial aging (20 h, 134 °C,

* *Corresponding author at*: Department of Prosthodontics and Periodontology, University of Sao Paulo, Bauru School of Dentistry, Al. Otavio Pinheiro Brisola 9-75, Bauru, SP, Brazil.
E-mail address: ernestobenalcazarj@gmail.com (E.B. Benalcazar Jalkh).
https://doi.org/10.1016/j.dental.2020.05.011

2.2 bar). Optical parameters were evaluated through repeated-measures analysis of variance and Tukey tests ($p < 0.05$). BFS data were analyzed using Weibull statistics (95% CI).
Results. High density values (95–99%) were found for all ceramic materials and SEM images exhibited a dense microstructure. While XRD patterns revealed the preservation of crystalline content in the ZTA composite, an increase in the monoclinic peak was observed for pure zirconias after aging. Significantly higher CR and lower TP values were observed for the ZTA composite, followed by alumina, 3YSB-E, and Zpex. The highest characteristic stress was recorded for 3YSB-E, followed by intermediate values between ZTA and Zpex, and the lowest for alumina. Aging affected the optical and mechanical properties of both zirconias, while remained stable for ZTA composite and alumina.
Significance. The synthesis of experimental 70−30% ZTA composite was successful and its relevance for dental applications relies on its higher masking ability, aging resistance, and strength similar to zirconia.

1. Introduction

Among the available ceramic materials in dentistry, yttrium-stabilized tetragonal zirconia polycrystals (3Y-TZP) has been broadly used for manufacturing infrastructures of single crowns [1,2] and fixed dental prostheses [3,4] for both tooth and implant-supported reconstructions. 3Y-TZP has also been indicated for bonded bridges [5], full arch implant supported prostheses [6], root posts [7], implant abutments [8], and dental implants [9].

3Y-TZP's capability of stress mediated phase transformation from tetragonal to monoclinic (t-m) phase, as a mechanism to resist the crack propagation in the core (transformation toughening) remains as one of its most interesting properties for load bearing applications [10]. When submitted to mechanical stress, zirconia grains around the crack tip undergoes a martensitic t-m transformation with a volumetric expansion of 3–5% of the grain size. Thus, the compressive stress produced during t-m transformation limits crack propagation increasing the fracture toughness of 3Y-TZP, a phenomenon known as R-curve behavior [11]. As a result, with a fracture toughness of 5−10 MPa and flexural strength greater than 1000 MPa [12], 3Y-TZP offers the highest mechanical properties among all ceramic materials along with excellent biocompatibility.

The highlighted mechanical properties of 3Y-TZP have led to a broad indication spectrum for long-span prostheses in dentistry, nevertheless clinical studies commonly do not involve follow ups longer than 10 years, but it has been reported that for long span applications including partial and full-arch fixed dental prostheses the survival rates are still lower than for metal ceramics, considered a gold-standard material [4]. Although the main issue reported in up to 5 year follow up studies is porcelain veneer cohesive fractures, known to be multifactorial [13], other problems have emerged as fatigue accumulates, including framework fractures, as reported in some clinical studies [14,15].

One important aspect that opens the field for innovations is the fact that zirconia is a metastable material where phase transformation may alter its properties. Within this context, variations in fabrication methods (like pressing method, sintering protocol, cooling rate and even milling parameters) [16–18] may lead to materials with varying properties. It has been reported, for instance, that phase transformation from tetragonal to monoclinic may vary from 2.13% to 81.4% in zirconia stabilized materials, as a function of variability in several parameters including microstructure, grain size, manufacturing and processing methods, along with laboratory aging protocols [19], suggesting that varying cumulative success rates from long-term clinical trials may be expected in the future also for framework survival [19,20].

Although 3Y-TZP was first introduced in Orthopedics in the 1990s for the manufacture of femoral head prostheses, the critical events in 2001 where hundreds of prostheses fractured due to an accelerated LTD process, raised concerns about long-term hydrothermal stability of zirconia [12]. For dental applications, zirconia also remains in direct contact with body fluids making it susceptible to tetragonal to monoclinic phase transformation due to stress and low temperature degradation (LTD) [21].

LTD process is accompanied by the appearance of micro cracks by the accumulation of stress within the material and the progressive loss of mechanical properties [22]. In addition, during the fabrication of porcelain fused to zirconia prostheses, moisture of the porcelain suspension and its subsequent heating during the sintering process have been shown to trigger tetragonal to monoclinic phase transformation of 3Y-TZP [23], which may compromise the porcelain stability due to increased residual stress [23,24]. Lastly, phase transformation at porcelain veneer/framework and intaglio surfaces may result in alterations in optical properties that may hamper long-term esthetic results, considering the role of the prostheses framework in the optical properties of the final bilayered restoration [25].

To improve the hydrothermal stability of 3Y-TZP at room temperature, the combination of zirconia particles within an alumina matrix has been proposed [26,27]. Zirconia toughened alumina (ZTA) are polycrystalline ceramic composites composed of an alumina matrix and a secondary phase of metastable tetragonal zirconia combining the advantageous properties of both materials [28]. Studies in orthopedics have revealed an increase in strength and fracture toughness of the

Table 1 – Composition of the 3Y-TZP powders (Zpex and TZ-3YSB-E; Tosoh Corporation).

	3Y-TZP powders chemical composition [wt.-%]						
	Particle size (nm)	Y_2O_3	Al_2O_3	Na_2O	SiO_2	FeO_2O_3	HfO_2
3YSB-E	90	5.35	≤0.1–0.4	≤0.04	≤0.02	≤0.01	<5.0
Zpex	40	5.2 ± 0.2	≤0.1	≤0.04	≤0.02	≤ 0.01	<5.0

Table 2 – Composition of high purity alumina powder (Baikalox Regular CR10).

Al powder composition									
	Particle size (nm)	Crystal structure		Chemical analyses ICP (ppm)					
		Alpha	Gamma	Fe	Na	Si	Ca	K	Mg, Ti, Cr, Mn, Ni, Cu, Zn
Baikalox Regular CR10	350	95%	5%	6	13	18	2	22	<1 each

composite material with little reduction in hardness and elastic modulus compared to monolithic alumina. In addition, the alumina matrix contributes to the stability of the tetragonal phase of zirconia by decreasing the LTD phenomena of 3Y-TZP [12,29].

As transformation mechanism propagates through the nucleation of a zirconia grain and the growth and transformation of neighboring grains, it has been suggested that the maximum fraction of zirconia in a ZTA composite to limit the propagation of the transformation is related to the interconnectivity of the zirconia grains within the alumina matrix [30].This fraction, known as percolation threshold, has been suggested to be up to 16% zirconia in 84% alumina matrix [30,31]. Nevertheless, studies on Y-TZP content between 15 and 30% have presented promising results for ZTA composites that encourage future investigation [32].

This study sought to develop a synthesis method for a ZTA composite in 70% Al_2O_3 and 30% Zr_2O and characterize its aging resistance along with possible changes in optical, mechanical and microstructural properties of ZTA after an accelerated aging protocol. We hypothesized that the formulated ZTA composite would be resistant to the accelerated aging protocol and that optical and mechanical properties would only be altered in the pure zirconia materials.

2. Materials and methods

2.1. *Experimental ceramic materials fabrication*

The four experimental groups were: (1) 3YSB-E: first generation 3Y-TZP with a particle size of 90 nm (TZ-3YSB-E, Tosoh Corporation, Tokyo, Japan); (2) Zpex: second generation 3Y-TZP with enhanced translucency when compared to first generation 3Y-TZP, with a particle size of 40 nm (Zpex, Tosoh Corporation); (3) alumina: high purity alumina with a particle size of 350 nm (α-Al_2O_3, Baikalox Regular CR10, Baikowski, Poisy, France); and (4) ZTA-Zpex: ZTA composite comprised by 70% alumina (α-Al_2O_3, Baikalox Regular CR10, Baikowski) and 30% zirconia (Zpex, Tosoh Corporation). The composition of the ceramic powders is detailed in Tables 1 and 2.

For alumina specimen synthesis, an ethanol suspension containing the high purity alumina powder, 1% of polyvinyl butyral binder (Sigma-Aldrich, St. Louis, Missouri, USA) and 500 ppm of magnesium oxide was prepared. The suspension was homogenized and mixed in a friction mill for 4 h using high-purity alumina spheres. The slurry was dried in rotary evaporator (801, Fisaton, São Paulo, Brazil) and the powders were manually granulated and sieved.

For ZTA composite synthesis, a suspension in ethanol containing alumina (70%) and zirconia (30%) powders were prepared. The suspension was homogenized and mixed, then the slurry was dried, and the powder was granulated and sieved as previously described for pure alumina powder.

Pure zirconia (3YSB-E and Zpex), alumina, and experimental ZTA powders were uniaxially pressed at 1148 kgf for 30 s in a tungsten carbide matrix with 15 mm of diameter to obtain disc shaped green body samples with 1.8 mm thickness. Green body samples were double wrapped and sealed in a vacuum sealer (Jumbo Plus, Globavac, Itajai, SC, Brazil) and subjected to isostatic pressing performed on cold isostatic press (National Forge, Irvine, PA, USA) at room temperature for 30 s at 30000 psi.

Samples were sintered at 1500°C (Zpex and 3Y-SBE) and 1600°C (Alumina and ZTA composite) for 1 h (Zyrcomat Furnace, Vita Zahnfabrink, Bad Säckingen, Germany) with heating and cooling rate of 4 °C per minute. Polishing of the two flat surfaces was performed in a semi-automatic polishing machine (Automet 2000, Buehler, Lake Buff, IL, USA) with 220, 120, 90, 40, 25, 15, 9, 6 and 1 μm granulated diamond disks (ALLIED High Tech Products, Rancho Dominguez, CA, USA) with diamond suspensions. Forty specimens with 12 mm of diameter and 1 mm thickness were prepared for optical and microstructural characterization (n = 10/per material), and two hundred and forty specimens with the same dimensions were prepared for mechanical characterization through biaxial flexural strength (BFS) test (n = 60/per material).

The following characterization tests were performed before and after autoclave accelerated artificial aging (20 h, 134°C, 2.2 bar).

2.2. *Density*

The relative density was determined based on the Archimedes' principle for all experimental materials after sintering. The density of the specimens was measured using an analytical balance (XS64 Analytical balance, Mettler Toledo, Columbus, OH, USA) and theoretical density kit accessory (Mettler Density Kit, Mettler Toledo, USA).

2.3. Scanning electron microscope (SEM)

The micromorphology of the experimental materials was analyzed at high-resolution Scanning Electron Microscope by Field Emission Gun (FEG-SEM) (MIRA3-TESCA, Brno-Kohoutovice, Czech Republic) with a secondary electron (SE) detector under magnification of 20,000× at 15–20 kV. Before evaluation, samples were submitted to thermal treatment at 1520 °C for Alumina and ZTA composites, and 1420 °C for Y-TZP specimens during one hour with heating and cooling rate of 4 °C per minute (Zyrcomat Furnace, Vita Zahnfabrink, Bad Säckingen, Germany). Subsequently, all samples were gold coated for 60 s at 20 mA (Quantum Sputter Q16OR ES).

2.4. Phase analysis

Crystalline spectra were determined for all experimental materials by X-ray diffraction (XRD, Miniflex, Rigaku, Tokyo, Japan). The scanning was performed on the Bragg θ-2θ geometry, equipped with a graphite monochromator and Cu Kα radiation (λ = 1.5406 Å), operating at a voltage of 40 kV and a current emission of 40 mA. Data were obtained in periods of 1.0 s and steps of 0.020 (2θ) of 10–80°. Baseline subtraction was performed in HighScore Plus Software (Malvern Panalytical Ltd, Westborough, Massachusetts, USA) for all XRD spectra. Monoclinic and tetragonal peaks were identified, and peaks intensity were recorded for monoclinic phase calculation. The monoclinic phase content (%) was quantified through formulas introduced by Toraya et al. [33], as follows: $Xm = \frac{[Im(-111)+Im(111)]}{[Im(-111)+Im(111)+It(101)]}$, where I_m (−111) and I_m (111) represents the monoclinic peaks intensity (2θ = 28° and 31.2°, respectively), and I_t (101) represents the intensity of the tetragonal peak (2θ = 30°); and, $Vm = 1.311 \times \left(\frac{Xm}{1}\right) + (0.311 \times Xm)$, where Vm represents the monoclinic volumetric content.

2.5. Optical properties

Ten specimens of each ceramic material were analyzed in spectrophotometer CM 3700d (Konica Minolta) that operates in the wavelengths range of visible light (400–700 nm). After cleaning in 80% isopropyl alcohol ultrasonic bath for 10 min, reflectance tests were performed over white (Yw) and black (Yb) backgrounds, and the values were used to determine the contrast ratio (CR) and translucency parameter (TP).

CR is the property that measures the transparency or opacity of materials by the ratio of the reflectance of the specimen over a black background (Yb) to the reflectance of the same specimen over a white background (Yw), which is given per: $CR = {}^{Y_b}/_{Y_w}$.

TP, which defines the masking ability of the material, was obtained by calculating the color difference (ΔE) of the specimens on black and white backgrounds, according to the equation: $\Delta E = \left[\left(L_b^* - L_w^*\right)^2 + \left(a_b^* - a_w^*\right)^2 + \left(b_b^* - b_w^*\right)^2\right]^{1/2}$. Where the subscripts b* (black) and w* (white) indicate the background color, and the coordinates L*, a*, and b* correspond to the lightness, chromaticity on the red/green axis, and chromaticity on the yellow/blue axis, respectively.

2.6. Biaxial flexural strength (BFS)

Sixty specimens of each material group were randomly divided for immediate and aged conditions (n = 30) for BFS test using a piston-on-three balls device, according to ISO 6872−2015. Testing was performed in an ElectroPuls™ E3000 Linear-Torsion (Instron, Norwood, MA, EUA) equipment at a crosshead speed of 0.5 mm/min until fracture. The maximum load was recorded for each specimen (N), and the following equations were used to calculate biaxial flexural strength (MPa):

$$\sigma = -0.2387P(X-Y)/b^2$$

$$X = (1+v)\mathrm{Ln}(r_2/r_3)^2 + ([1-v]/2)(r_2/r_3)^2$$

$$Y = (1+v)[1+\mathrm{Ln}(r_1/r_3)^2] + (1-v)(r_1/r_3)^2$$

where, σ = biaxial flexural strength (MPa), P = fractured load (N), b = disk specimen thickness at fracture site (1.2 ± 0.2 mm), v = Poisson ratio (0.25), r_1 = radius of support circle (5.5 mm), r_2 = radius of loaded area (0.75 mm), and r_3 = radius of the specimen (6 mm).

The fractured specimens were examined in Axio Zoom V16 Stereo Zoom Microscope (Carl Zeiss, Oberkochen, Germany) to assess fractographic marks evidence of the fracture origin and direction of propagation.

2.7. Low-temperature aging

Low-temperature degradation (LTD) was simulated in an autoclave (Vitale Class CD, Cristofoli, Campo Mourão, PR, Brazil) at 134 °C, under a 2.2 bar pressure, over a period of 20 consecutive hours. [19]

2.8. Statistical analysis

Data from optical properties were tabulated and subjected to descriptive analysis, normality and homoscedasticity test. Data normality and homoscedasticity were confirmed using Shapiro–Wilk ($p > 0.05$) and Levene ($p > 0.25$) tests. Repeated-measures analyses of variance and Tukey tests were used for statistical evaluation of CR and TP differences with an overall significance level of 5% at Minitab 17 statistical software (Minitab Inc. PA, USA). Data are presented as a function of mean values and standard deviation. Biaxial flexural strength data were analyzed using Weibull 2-parameter distribution (Synthesis 9, Weibull ++9, Reliasoft, Tucson, AZ, USA). Weibull parameters [characteristic stress (MPa) and Weibull modulus (m)] were calculated, and a contour plot was graphed to determine differences between groups. The probability of survival as function of characteristic stress were calculated to stresses of 300, 500, and 800 MPa, which are the ISO 6872:2015 required stress for 3-unit anterior substructures (up to premolar, class 3 ceramics), 3-unit posterior substructures (class 4 ceramics), and 4-unit or larger span substructures for fixed dental prostheses (FDP), respectively.

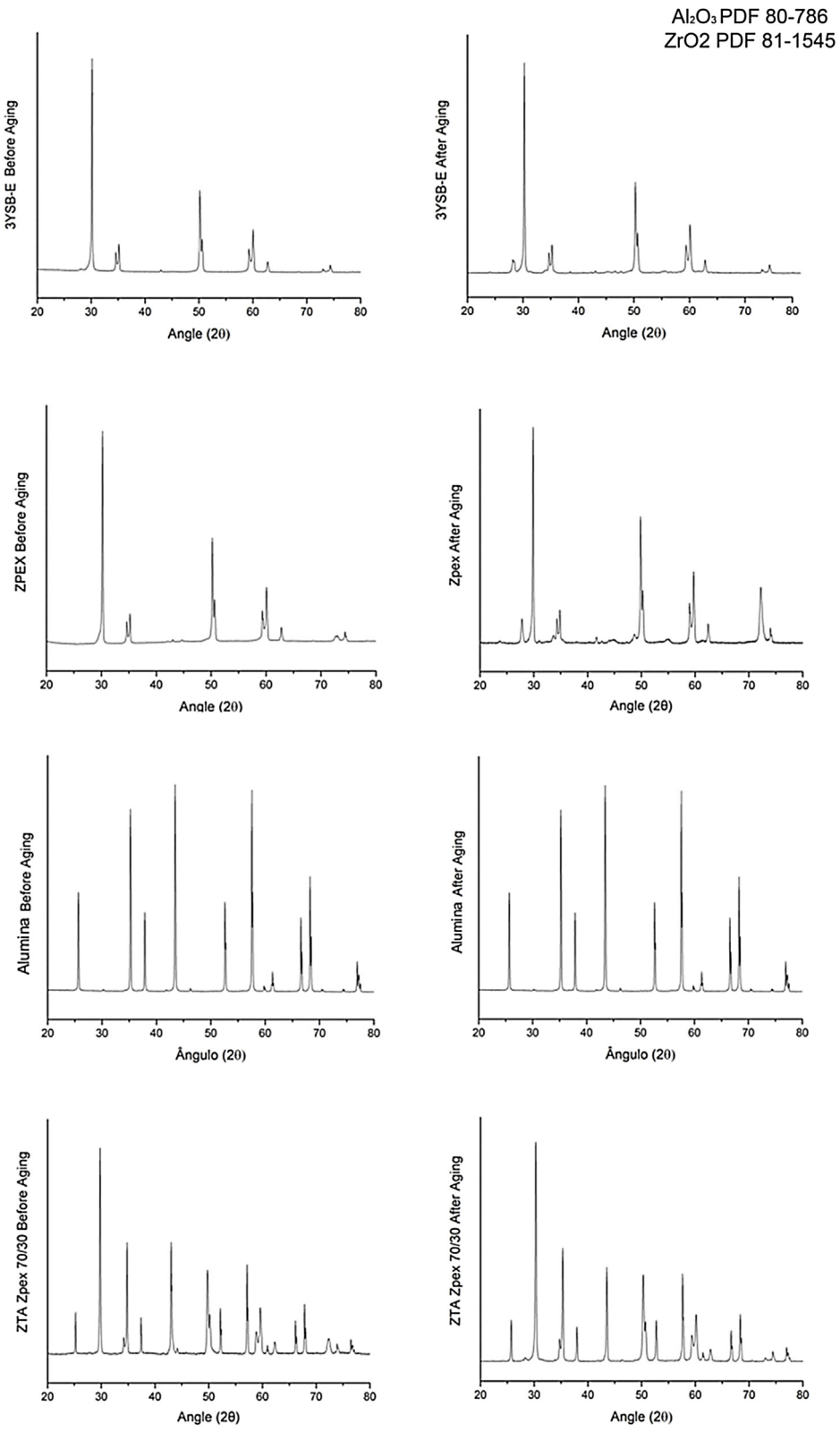

Fig. 1 – XRD patterns of 3YSB-E, Zpex, Alumina and ZTA-Zpex before and after aging.

Table 3 – Density of sintered discs based on Archimedes' principle.

Material	Density (%)
3YSB-E	98.72 (±0.2)
Zpex	98.61 (±0.2)
Alumina	98.93 (±0.3)
ZTA-Zpex	95.34 (±0.2)

Table 4 – Monoclinic phase content of experimental materials before and after aging.

Material	Monoclinic phase %	
	Before aging	After aging
3YSB-E	1.2	8.5
Zpex	1.7	23.6
ZTA-Zpex	1.3	3.3

3. Results

The densities of the sintered specimens ranged from 95 to 99% according to the Archimedes' principle to all experimental materials (Table 3).

The X-ray diffraction (XRD) spectra of all materials were plotted and typical alumina and zirconia peaks could be identified, and the monoclinic crystalline content quantified, as demonstrated in Fig. 1 and Table 4. Alpha alumina (α-Al_2O_3) peaks, as well as, cubic (Zc), tetragonal (Z_T) and monoclinic (Z_M) zirconia peaks were detected. XRD spectra analyses indicated a slight percentage of monoclinic phase in the as-sintered materials (all, approximately 1.5%). While the monoclinic content was stable after artificial aging in the ZTA composite (3.3%), tetragonal-to-monoclinic transformation and increased percentage of monoclinic phase could be observed in the Zpex (23.5%) and 3YSB-E (8.5%).

Scanning electron microscopy (SEM) micrographs, illustrated in Fig. 2, depicted the micromorphological characterization of the experimental materials before and after aging. A dense surface was obtained for ZTA composite, which was similar to the control materials (zirconia and alumina). Moreover, a uniform distribution of the zirconia disperse phase within the alumina matrix can be observed. Alumina showed a smaller particle size in the composite related to the pure composition, different from zirconia that exhibited a similar grain growth in the pure and composite formulations. By comparison, both zirconia and alumina particles were spherical and dense with few microstructural pores and defects distributed along the ceramic surface, which may be related to the ceramic processing.

Tables 5 and 6 summarize the contrast ratio (CR) and translucency parameter (TP) values, respectively, calculated for each experimental material. The CR that measures the translucency or opacity of the material showed lower values for the Zpex group (0.77 ± 0.05), followed by 3YSB-E (0.85 ± 0.046), and alumina groups (0.96 ± 0.02), all pairwise comparisons were significantly different ($p < 0.001$). ZTA composite, ZTA-Zpex (1.00 ± 0.006) presented significantly higher CR values when compared to pure alumina and zirconia formulations ($p < 0.001$). After aging, corresponding statistical differences were observed for the ceramic materials CR values.

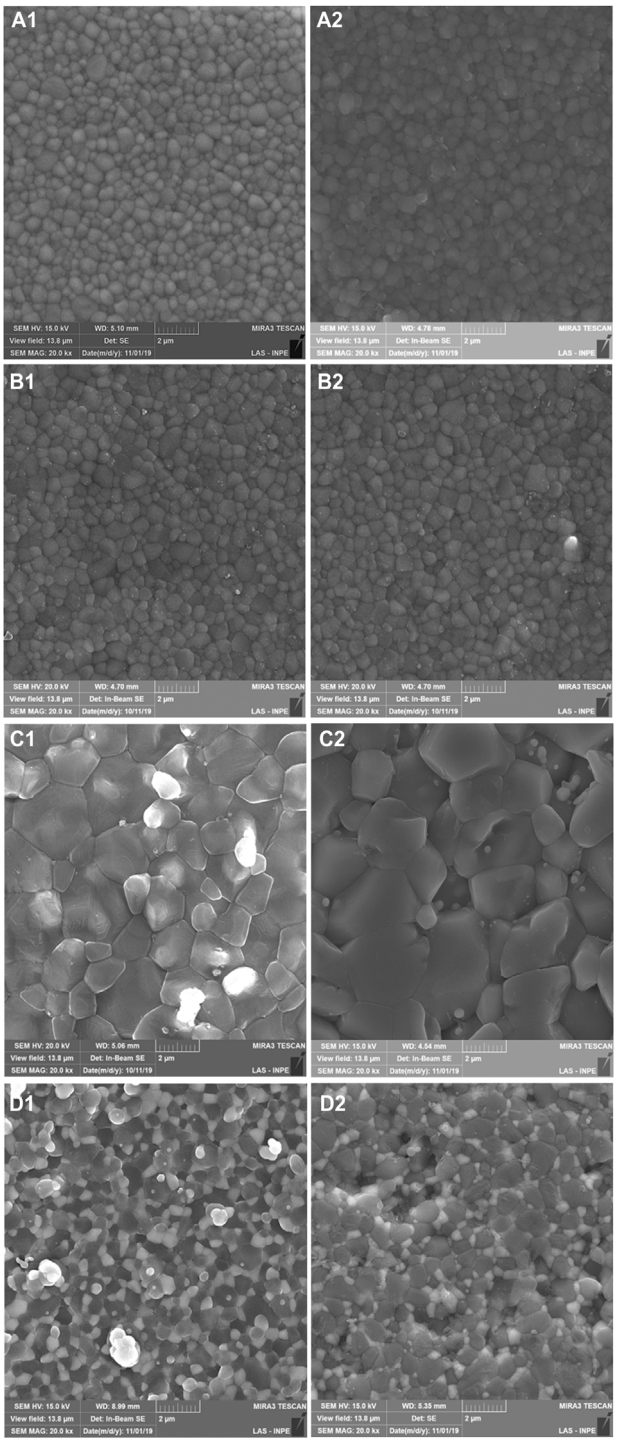

Fig. 2 – SEM images of all ceramic groups represented by letters A–E as follows: (A) 3YSB-E, (B) Zpex, (C) Alumina and (D) ZTA/Zpex. Numbers 1 and 2 represents the as sintered and aged conditions respectively.

Nonetheless, while ZTA composite (0.99 ± 0.001) and alumina (0.95 ± 0.02) CR values remained stable after artificial aging ($p > 0.308$), pure zirconia systems exhibited significantly lower CR values (Zpex: 0.68 ± 0.07 and 3YSB-E:0.79 ± 0.046) ($p < 0.001$).

TP that describes the translucency and masking ability of the material showed higher values for Zpex group (10.23 ±

Table 5 – Mean contrast ratio (CR) and standard deviation of each experimental ceramic material.

Material	Contrast ratio	
	Immediate	Aged
3YSB-E	0.85 (0.046)^{Aa}	0.79 (0.046)^{Ab}
ZPEX	0.77 (0.05)^{Ba}	0.68 (0.07)^{Bb}
Alumina	0.96 (0.02)^{Ca}	0.95 (0.02)^{Ca}
ZTA Zpex	1.00 (0.006)^{Da}	0.99 (0.001)^{Da}

Different uppercase letters indicate statistical difference between materials and different lowercase letters indicate statistical difference before and after aging.

Table 6 – Mean translucency parameter (TP) with respective standard deviation of each material.

Material	Translucency parameter	
	Immediate	Aged
3YSB-E	7.13 (0.23)^{Aa}	9.70 (1.79)^{Ab}
ZPEX	10.23 (0.41)^{Ba}	15.51 (0.62)^{Bb}
Alumina	2.39 (0.35)^{Ca}	2.53 (0.53)^{Ca}
ZTA Zpex	0.24 (0.12)^{Da}	0.42 (0.26)^{Da}

Different uppercase letters indicate statistical difference between materials and different lowercase letters indicate statistical difference before and after aging.

0.41), followed by 3YSB-E (7.13 ± 0.23), and alumina groups (2.38 ± 0.35), all pairwise comparisons were significantly different ($p < 0.001$). ZTA composite (0.24 ± 0.12) presented significantly lower TP values and higher masking ability when compared to pure alumina and zirconia formulations ($p < 0.001$). After aging, corresponding statistical differences were observed for the ceramic materials TP values. Nonetheless, while ZTA composite (0.42 ± 0.26) and alumina (2.53 ± 0.53) CR values remained stable after artificial aging ($p > 0.544$), pure zirconia systems exhibited significantly higher TP values (Zpex: 15.51 ± 0.62 and 3YSB-E:9.70 ± 1.79) ($p < 0.001$).

Table 7 summarizes the results of the mechanical properties of all tested groups. Weibull parameters characteristic stress (MPa) and Weibull Modulus (*m*)] are presented as a function of 95% confidence interval before and after aging. Weibull modulus, used as a measure that expresses the structural reliability of the material, and characteristic stress, which represents the stress at a failure probability of approximately 63.2%, evidenced no statistical difference between immediate and aged ZTA polycrystalline composite as demonstrated by the overlap of contours in the Contour plot (Fig. 3). The

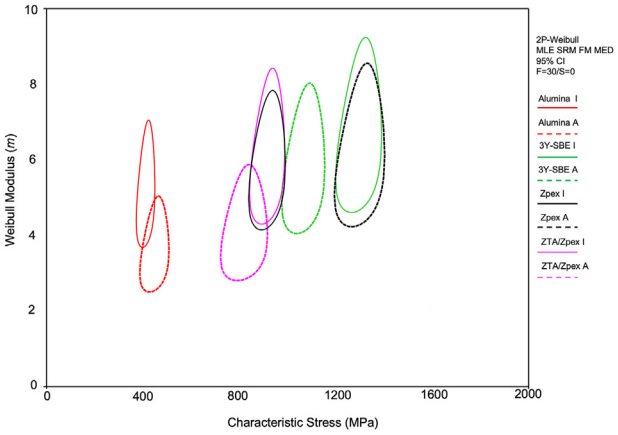

Fig. 3 – Contour plot showing the relationship between Weibull modulus (m) and characteristic stress (MPa). Overlapping between contour graphs indicates no statistical difference between groups (95% CI).

highest characteristic stress among all immediately tested groups was recorded for 3YSB-E, which decreased significantly after aging. Zpex and ZTA-Zpex tested before aging presented similar characteristic stress values, both significantly lower than immediate 3YSB-E as depicted in Fig. 3 by the overlapping of the contour plots. After aging, 3YSB-E presented a significant decrease in characteristic stress, while values significantly increased for Zpex, which in this condition significantly surpassed the values of aged 3YSB-E. ZTA-Zpex composite characteristic stress values did not alter significantly after aging. Finally, pure Alumina presented the lowest characteristic stress among all tested groups and also remained stable after aging. No significant differences in Weibull modulus was observed among all immediate and aged tested groups. The use level probability Weibull plot presented in the Fig. 4 shows the failure distribution of samples as a function of stress.

The probability of survival of the experimental ZTA composite was estimated at approximately 100% for 300 and 500 MPa, however, a significant decrease was demonstrated for immediate and aged ZTA at 800 MPa. For all estimated stress values, aging did not affect the probability of survival of the ZTA composite. 3YSB-E presented a probability of survival of approximately 100% for all stress calculations, however, aging produced a significant decrease (up to 20%) in its probability of survival at 800 MPa. Zpex evidenced high probability

Table 7 – Mean Weibull modulus and characteristic stress (MPa) results with the corresponding 95% CI.

	Weibull modulus (m)		Characteristic stress (MPa)	
	Immediate	Aged	Immediate	Aged
3Y-SBE	6.7 Aa (5.3–8.5)	5.9 Aa (4.7–7.4)	1294 Aa (1234–1356)	1063 Bb (1008–1122)
Zpex	5.9 Aa (4.8–7.3)	6.2 Aa (4.9–7.8)	913 Ab (865–963)	1297 Ba (1232–1365)
Alumina	5.3 Aa (4.2–6.5)	3.7 Aa (2.9–4.6)	410 Ac (386–436)	445 Ad (408–486)
ZTA-Zpex	6.2 Aa (5–7.8)	4.2 Aa (3.3–5.4)	914 Ab (869–962)	815 Ac (756–879)

Uppercase letters denote statistically significant differences between immediate and aged conditions. Lowercase letters denote significant differences between materials.

Table 8 – Reliability and the respective 95% confidence intervals (CI).

	300 MPa		500 MPa		800 MPa	
	Immediate	Aged	Immediate	Aged	Immediate	Aged
3Y-SBE	1.0 Aa (1.0–1.0)	1.0 Aa (1.0–1.0)	1.0 Aa (0.99–1.0)	0.99 Aa (0.96–1.0)	0.96 Aa (0.91–0.98)	0.83 Ba (0.72–0.9)
Zpex	1.0 Aa (0.99–1.0)	1.0 Aa (1.0–1.0)	0. 97Aa (0.93–0.99)	1.0 Aa (0.99–1.0)	0.63 Ab (0.5–0.74)	0.95 Ba (0.89–0.98)
Alumina	0.82 Ab (0.72–0.89)	0.79 Ab (0.67–0.87)	0.06 Ab (0.02–0.13)	0.22 Ac (0.13–0.32)	0 Ac (0–0)	0 Ac (0–0)
ZTA-Zpex	1.0 Aa (0.99–1.0)	0.99 Aa (0.95–1.0)	0.98 Aa (0.94–0.99)	0.88 Ab (0.78–0.94)	0.65 Ab (0.52–0.75)	0.4 Ab (0.28–0.52)

Uppercase letters denote statistically significant differences between immediate and aged conditions. Lowercase letters denote significant differences between materials.

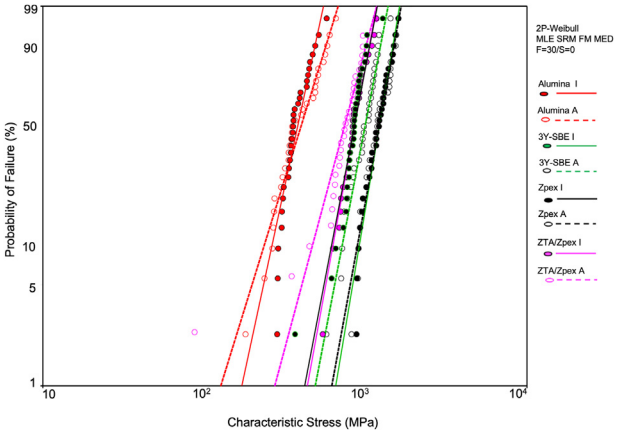

Fig. 4 – Use level probability Weibull curves show sample failure distribution as a function of stress.

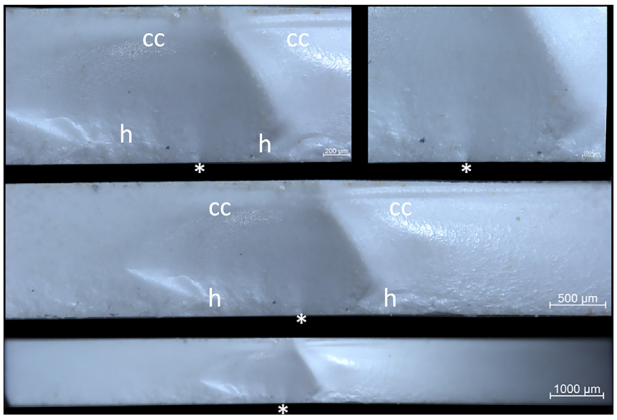

Fig. 5 – Stereomicroscope images of a representative fractured surface. The bottom central area of the fragment shows the presence of a flaw in the area subjected to maximum tensile stress, where fractographic marks, such as hackle lines (h) and compression curls (cc), indicate the fracture origin (asterisk) and propagation to the compression side of the discs.

of survival (~100%) at 300 and 500 MPa, nevertheless a significant decrease (up to 37%) was observed at 800 MPa. The increase in characteristic stress produced by aging determined an increase in the probability of survival of aged Zpex for missions at 800 MPa (95%). Finally, Alumina presented the lowest probability of survival among all immediate and aged groups (Table 8).

Fractographic marks, including hackle lines and compression curls, were used to suggest the origin of the fracture, generally related to tensile side defects originated during the processing of the ceramic specimens, which propagated to the compression side of disc (Fig. 5).

4. Discussion

This study sought to synthesize a zirconia toughened alumina (ZTA) composite with 70% alumina reinforced by 30% of a second generation 3Y-TZP (Zpex), and to characterize its microstructure, crystalline content, optical and mechanical properties before and after aging for comparison with the respective zirconia and alumina isolated counterparts, as well as with a first generation 3Y-TZP indicated as framework material. In fact, the synthesis of the experimental 70–30% ZTA composite was successful and resulted in a dense microstructure with uniform distribution of the zirconia disperse phase within the alumina matrix. While crystalline content, optical and mechanical properties of the ZTA composite and alumina remained stable after artificial aging, zirconia materials presented increased percentage of monoclinic phase and alteration in the optical and mechanical evaluated parameters. Thus, the postulated hypothesis that the formulated ZTA composite would be resistant to the accelerated aging protocol and that optical and mechanical properties would only be altered in the pure zirconia systems was accepted.

Zirconia LTD has been extensively studied in orthopedics since its detrimental effects have shown to risk prostheses survival, especially in total hip arthroplasties [21,26,34]. In dentistry, it has been recently reported that some first and second generation zirconias do show t-m transformation, after only 100 days in the oral environment, which impacted not only their mechanical properties but also increased their surface roughness [35]. The clinical impact of these findings in restorative dentistry is yet to be determined in long-term clinical trials of 10 or more years, but it seems reasonable to encourage the development of all-ceramic framework materials that are stable, as proposed over a decade ago in the orthopedic field [26].

Furthermore, as monoclinic and tetragonal zirconia crystals are birefringent, meaning that the index of refraction is anisotropic in the different crystallographic directions, LTD alters the optical properties of dental zirconia over time since a discontinuity of the refractive index at the grain boundaries affects light transmission [36,37]. To overcome the concerns

related to long-term stability of the mechanical and optical properties of 3Y-TZP, we have proposed a 70–30% ZTA composite synthesized with high purity alumina and a second generation 3Y-TZP (ZTA-Zpex) for dental applications [33]. The XRD spectra analysis and monoclinic phase percentage calculation in the present study revealed the stability of the tetragonal phase of the ZTA composite after aging. Previous studies from our group have recently shown that 80/20% and 85/15% ZTA composites, also presented stable crystalline phases that were unaffected by artificial aging [38,39]. This behavior may lie on the limited interconnectivity of zirconia grains by the alumina matrix in ZTA composite, with an interruption of the nucleation and growth mechanism associated with LTD [40].

Conversely, pure zirconia groups (Zpex and 3YSB-E) presented a significant tetragonal to monoclinic phase transformation (23.6% and 8.5% respectively). The monoclinic percent difference between both materials might be associated with the alumina dopant content, 0.1 and 0.4% for Zpex and 3YSB-E, respectively. Aluminum oxide is commonly added as a dopant agent to pure zirconia to promote additional tetragonal phase stabilization [36]. Nonetheless, to enhance the translucency of second-generation 3Y-TZP monolithic zirconia systems, as Zpex, alumina content has been reduced to up to 0.1% and the higher hydrothermal instability was already expected. Moreover, it was previously reported that the larger the grain size, the more prone to tetragonal-to-monoclinic transformation during aging the zirconia becomes [41,42].

Despite the higher contrast ratio (CR) and lower translucency parameter (TP) values obtained for the ZTA composite relative to the alumina and zirconia materials, laboratory autoclave aging has not affected the stability of its optical properties. Many factors have been associated with the optical properties and light-scattering mechanism of polycrystalline systems, including the birefringent nature of crystals and scattering of light at grain boundaries, grain size, pores, the inclusion of a second-phase particles (as in the ZTA composites), and surface roughness [36,43,44]. Based on such assumptions, it can be speculated that the higher opacity and masking ability of the ZTA composite in comparison to the alumina and zirconia materials lies on the refractive index mismatch between the two phases and crystallography that hampers light transmission, as well as, on the presence of pores and defects associated with ceramic processing [36,45]. The maintenance of the ZTA optical parameters values after artificial aging may be related to the stability of the crystalline content and microstructure due to the higher hardness of alumina and limited interconnectivity of zirconia grains that limits zirconia phase transformation [12]. Due to its high masking ability, one of ZTA dental applications would be as a surrogate for metal frameworks in clinical scenarios where masking of darkened substrates such as colored teeth or titanium implant abutments are required [46].

Laboratory autoclave aging has affected the stability of the optical properties of zirconia groups. The increased translucency of the Zpex and 3YSB-E after aging may be attributed to a favored light transmission as a consequence of the crystalline morphology rearrangement (crystal phase, size and shape), as well as, the possible sealing of pores and defects as a result of the volumetric expansion associated with tetragonal-to-monoclinic phase transformation [36,44], as shown in the XRD spectra and SEM images. Moreover, the significant difference in the CR and TP for both zirconia systems, Zpex and 3YSB-E, may lie on the higher alumina dopant content of conventional zirconia, grain size and, consequently, higher susceptibility to LTD. In contrast, some studies have shown a decreased translucency of zirconia ceramic after autoclave aging [45,47], which may suggest that optical changes in dental zirconias might be related not only to their composition, microstructure, and crystalline content, but also to the simulated hydrothermal aging protocol [48]. While initial tetragonal-to-monoclinic phase transformation has been associated with defects sealing favoring light transmission, a progressive transformation may generate defects and increase the superficial roughness that intensifies light scattering [40].

The results of the experimental ZTA and pure zirconias mechanically tested in the present study revealed a Weibull modulus that ranged from approximately 5–8 with no statistical difference between groups and within the range of values reported for the currently available ceramic systems [49]. The higher the Weibull modulus, the more homogeneous the flaw size distribution and the less the data scatter and, therefore, greater structural reliability [50,51].

The ZTA composite synthesized in the present study evidenced mechanical performance (~914 MPa) significantly higher than pure alumina (~400 MPa) and similar to previous reported data for different commercially available dental Y-TZPs (817–1121 MPa) [52,53]. Although predominantly composed of alumina, the high mechanical performance of the ZTA composite may be explained by the zirconia reinforcement volume, the dense microstructure with homogeneous distribution of zirconia and alumina grains, as well as toughening mechanisms, including stress-induced phase transformation that hinders crack propagation and crack deflection through residual compressive stress resulting from the thermal expansion mismatch of the two crystalline phases [39,54]. These findings are compatible with published literature on the orthopedic field, where advantageous flexural strength for ZTA composites with reinforcements up to 20 and 30% of zirconia particles has been reported (~1000 MPa) [54].

3YSB-E group, a first-generation 3Y-TZP, presented the highest mechanical performance among the tested groups (~1294 MPa), however, accelerated aging in autoclave produced a significant strength reduction (~1063 MPa). Such a decrease may be due to the volumetric alterations caused by t-m phase transformation of zirconia grains, which may have led to tension accumulation to reach the critical value, compromising the microstructural integrity of 3YSB-E [22,34,55]. On the other hand, Zpex, a second-generation 3Y-TZP, that exhibited characteristic stress similar to the ZTA composite (~913 MPa), presented a significant increase in mechanical performance after aging (~1297 MPa). It can be hypothesized that zirconia t-m phase transformation and volume expansion led to the accumulation of compressive stress [55,56], therefore, the volumetric increase of the grains might have been insufficient to reach the critical tension that would lead to the collapse of the grains, increase the population of defects in the material, and reduce the flexural strength [42].

The probability of survival of the experimental ZTA composite estimated at 100% and 98% for 300 and 500 MPa

stresses respectively makes the experimental material an interesting alternative for anterior and posterior three-unit FDP frameworks according to ISO 6872:2015 biaxial flexural strength recommendation for fixed dental prostheses. The high masking ability and excellent hydrothermal stability provide promising advantages for ZTA composite as infrastructure material when compared to first and second generation 3Y-TZPs, and less challenging from an esthetic perspective when compared to metallic frameworks. Nevertheless, different compositions and syntheses protocols should be developed to improve the strength and reliability for 4-unit or larger span FDP frameworks, where the probability of survival of the ZTA composite at 800 MPa presented a significant decrease (52–75%). 3YSB-E presented high probability of survival (~96–100%) for stresses at 300, 500, and 800 MPa, however a significant decrease (~20%) was observed at 800 MPa after aging, which sustain the concerns about LTD in pure zirconia submitted to low temperatures, stress and humid conditions. Although Zpex presented similar mechanical behavior than the ZTA composite in the immediate condition, a significant improve in the probability of survival was observed after aging. Although this behavior seems interesting from a mechanical perspective, the changes produced by LTD on zirconia grains led to several optical and microstructural alterations that may compromise the final esthetic outcomes of monolithic prosthetic treatments manufactured with this second-generation 3Y-TZP, especially in the long term. Testing these materials for fatigue performance is paramount to comprehensively characterize their lifetime.

5. Conclusion

ZTA composite exhibited significantly higher masking ability, and its optical and mechanical properties did not vary after aging when compared to pure zirconia groups.

Acknowledgements

To São Paulo Research Foundation (FAPESP), grant # 2012/19078-7, EMU 2016/18818-8, and scholarships # 2018/03072-6; 2019/00452-5; 2019/08693-1; 2016/17793-1 and 2017/19362-0. To Conselho Nacional de Desenvolvimento Científico e Tecnológico (CNPq), Grant # 304589/2017-9 and 434487/2018-0, to CAPES Financial Code 001. And to Secretaria Nacional de Educación Superior, Ciencia, Tecnología e Innovación (SENESCYT).

REFERENCES

[1] Sailer I, Makarov NA, Thoma DS, Zwahlen M, Pjetursson BE. All-ceramic or metal-ceramic tooth-supported fixed dental prostheses (FDPs)? A systematic review of the survival and complication rates. Part I: single crowns (SCs). Dent Mater 2015;31:603–23.

[2] Sailer I, Makarov NA, Thoma DS, Zwahlen M, Pjetursson BE. Corrigendum to "All-ceramic or metal-ceramic tooth-supported fixed dental prostheses (FDPs)? A systematic review of the survival and complication rates. Part I: single crowns (SCs)" [Dental Materials 31 (6) (2015) 603–623]. Dent Mater 2016;32:e389–90.

[3] Pjetursson BE, Sailer I, Makarov NA, Zwahlen M, Thoma DS. All-ceramic or metal-ceramic tooth-supported fixed dental prostheses (FDPs)? A systematic review of the survival and complication rates. Part II: multiple-unit FDPs. Dent Mater 2015;31:624–39.

[4] Pjetursson BE, Sailer I, Makarov NA, Zwahlen M, Thoma DS. Corrigendum to "All-ceramic or metal-ceramic tooth-supported fixed dental prostheses (FDPs)? A systematic review of the survival and complication rates. Part II: multiple-unit FDPs" [Dental Materials 31 (6) (2015) 624–639]. Dent Mater 2017;33:e48–51.

[5] Sasse M, Kern M. CAD/CAM single retainer zirconia-ceramic resin-bonded fixed dental prostheses: clinical outcome after 5 years. Int J Comput Dent 2013;16:109–18.

[6] Larsson C, Vult Von Steyern P. Implant-supported full-arch zirconia-based mandibular fixed dental prostheses. Eight-year results from a clinical pilot study. Acta Odontol Scand 2013;71:1118–22.

[7] Paul SJ, Werder P. Clinical success of zirconium oxide posts with resin composite or glass-ceramic cores in endodontically treated teeth: a 4-year retrospective study. Int J Prosthodont 2004;17:524–8.

[8] Ferrari M, Vichi A, Zarone F. Zirconia abutments and restorations: from laboratory to clinical investigations. Dent Mater 2015;31:e63–76.

[9] Jung RE, Grohmann P, Sailer I, Steinhart YN, Feher A, Hammerle C, et al. Evaluation of a one-piece ceramic implant used for single-tooth replacement and three-unit fixed partial dentures: a prospective cohort clinical trial. Clin Oral Implants Res 2015;27:751–61.

[10] Garvie RC, Hannink RH, Pascoe RT. Ceramic steel. Nature 1975;258:703–4.

[11] Kelly JR, Denry I. Stabilized zirconia as a structural ceramic: an overview. Dent Mater 2008;24:289–98.

[12] Chevalier J, Gremillard L. Ceramics for medical applications: a picture for the next 20 years. J Eur Ceram Soc 2009;29:1245–55.

[13] Swain MV. Unstable cracking (chipping) of veneering porcelain on all-ceramic dental crowns and fixed partial dentures. Acta Biomater 2009;5:1668–77.

[14] Taskonak B, Yan J, Mecholsky Jr JJ, Sertgoz A, Kocak A. Fractographic analyses of zirconia-based fixed partial dentures. Dent Mater 2008;24:1077–82.

[15] Sailer I, Balmer M, Husler J, Hammerle CHF, Kanel S, Thoma DS. 10-year randomized trial (RCT) of zirconia-ceramic and metal-ceramic fixed dental prostheses. J Dent 2018;76:32–9.

[16] Paula VG, Lorenzoni FC, Bonfante EA, Silva NR, Thompson VP, Bonfante G. Slow cooling protocol improves fatigue life of zirconia crowns. Dent Mater 2015;31:77–87.

[17] Guess PC, Bonfante EA, Silva NR, Coelho PG, Thompson VP. Effect of core design and veneering technique on damage and reliability of Y-TZP-supported crowns. Dent Mater 2013;29:307–16.

[18] Silva NR, Bonfante EA, Rafferty BT, Zavanelli RA, Rekow ED, Thompson VP, et al. Modified Y-TZP core design improves all-ceramic crown reliability. J Dent Res 2011;90:104–8.

[19] Pereira GK, Venturini AB, Silvestri T, Dapieve KS, Montagner AF, Soares FZ, et al. Low-temperature degradation of Y-TZP ceramics: a systematic review and meta-analysis. J Mech Behav Biomed Mater 2015;55:151–63.

[20] Pereira GK, Muller C, Wandscher VF, Rippe MP, Kleverlaan CJ, Valandro LF. Comparison of different low-temperature aging protocols: its effects on the mechanical behavior of Y-TZP ceramics. J Mech Behav Biomed Mater 2016;60:324–30.

[21] Chevalier J, Cales B, Drouin JM. Low-temperature aging of Y-TZP ceramics. J Am Ceram Soc 1999;82:2150–4.

[22] Chevalier J, Gremillard L, Virkar AV, Clarke DR. The tetragonal-monoclinic transformation in zirconia: lessons learned and future trends. J Am Ceram Soc 2009;92:1901–20.
[23] Tholey MJ, Berthold C, Swain MV, Thiel N. XRD2 micro-diffraction analysis of the interface between Y-TZP and veneering porcelain: role of application methods. Dent Mater 2010;26:545–52.
[24] Fukushima KA, Sadoun MJ, Cesar PF, Mainjot AK. Residual stress profiles in veneering ceramic on Y-TZP, alumina and ZTA frameworks: measurement by hole-drilling. Dent Mater 2014;30:105–11.
[25] Pires LA, Novais PM, Araujo VD, Pegoraro LF. Effects of the type and thickness of ceramic, substrate, and cement on the optical color of a lithium disilicate ceramic. J Prosthet Dent 2017;117:144–9.
[26] Chevalier J. What future for zirconia as a biomaterial? Biomaterials 2006;27:535–43.
[27] Fabbri P, Piconi C, Burresi E, Magnani G, Mazzanti F, Mingazzini C. Lifetime estimation of a zirconia-alumina composite for biomedical applications. Dent Mater 2014;30:138–42.
[28] Gracis S, Thompson VP, Ferencz JL, Silva NR, Bonfante EA. A new classification system for all-ceramic and ceramic-like restorative materials. Int J Prosthodont 2015;28:227–35.
[29] Jiang L, Liao Y, Wang C, Lu J, Zhang J. Low temperature degradation of alumina-toughened zirconia in artificial saliva. J Wuhan Univ Technol Sci Ed 2013;28:844–8.
[30] Pecharromán C, Bartolomé JF, Requena J, Moya JS, Deville S, Chevalier J, et al. Percolative mechanism of aging in zirconia-containing ceramics for medical applications. Adv Mater 2003;15:507–11.
[31] Ueno M. General manager, quality assurance corporate division: Japan medical materials; 2012.
[32] Casellas D, Rafols I, Llanes L, Anglada M. Fracture toughness of zirconia–alumina composites. Int J Refract Met Hard Mater 1999;17:11–20.
[33] Toraya H, Yoshimura M, Somiya S. Calibration curve for quantitative-analysis of the monoclinic-tetragonal ZrO_2 system by X-ray-diffraction. J Am Ceram Soc 1984;67.C119–C121.
[34] Chevalier J, Gremillard L, Deville S. Low-temperature degradation of zirconia and implications for biomedical implants. Annu Rev Mater Res 2007;37:1–32.
[35] Borges MAP, Alves MR, dos Santos HES, dos Anjos MJ, Elias CN. Oral degradation of Y-TZP ceramics. Ceram Int 2019;45:9955–61.
[36] Zhang Y. Making yttria-stabilized tetragonal zirconia translucent. Dent Mater 2014;30:1195–203.
[37] Zhang Y, Lawn BR. Novel zirconia materials in dentistry. J Dent Res 2017:22034517737483.
[38] Lopes ACO, Coelho PG, Witek L, Jalkh EBB, Gênova LA, Monteiro KN, et al. Nanomechanical and microstructural characterization of a zirconia-toughened alumina composite after aging. Ceram Int 2019;45:8840–6.
[39] Benalcazar Jalkh EB, Bergamo ETP, Monteiro KN, Cesar PF, Genova LA, Lopes ACO, et al. Aging resistance of an experimental zirconia-toughened alumina composite for large span dental prostheses: optical and mechanical characterization. J Mech Behav Biomed Mater 2020;104:103659.
[40] Chevalier J, Grandjean S, Kuntz M, Pezzotti G. On the kinetics and impact of tetragonal to monoclinic transformation in an alumina/zirconia composite for arthroplasty applications. Biomaterials 2009;30:5279–82.
[41] Lucas TJ, Lawson NC, Janowski GM, Burgess JO. Effect of grain size on the monoclinic transformation, hardness, roughness, and modulus of aged partially stabilized zirconia. Dent Mater 2015;31:1487–92.
[42] Prado P, Monteiro JB, Campos TMB, Thim GP, de Melo RM. Degradation kinetics of high-translucency dental zirconias: mechanical properties and in-depth analysis of phase transformation. J Mech Behav Biomed Mater 2019;102:103482.
[43] Kim MJ, Ahn JS, Kim MJH, Kim HY, Kim WC. Effects of the sintering conditions of dental zirconia ceramics on the grain size and translucency. J Adv Prosthodont 2013;5:161–6.
[44] Pekkan G, Pekkan K, Bayindir BC, Ozcan M, Karasu B. Factors affecting the translucency of monolithic zirconia ceramics: a review from materials science perspective. Dent Mater J 2019;39:1–8.
[45] Walczak K, Meissner H, Range U, Sakkas A, Boening K, Wieckiewicz M, et al. Translucency of zirconia ceramics before and after artificial aging. J Prosthodont 2019;28:e319–24.
[46] Fehmer V, Muhlemann S, Hammerle CH, Sailer I. Criteria for the selection of restoration materials. Quintessence Int 2014;45:723–30.
[47] Kurt M, Turhan Bal B. Effects of accelerated artificial aging on the translucency and color stability of monolithic ceramics with different surface treatments. J Prosthet Dent 2019;121:712.e1–8.
[48] Putra A, Chung KH, Flinn BD, Kuykendall T, Zheng C, Harada K, et al. Effect of hydrothermal treatment on light transmission of translucent zirconias. J Prosthet Dent 2017;118:422–9.
[49] Tinschert J, Zwez D, Marx R, Anusavice KJ. Structural reliability of alumina-, feldspar-, leucite-, mica- and zirconia-based ceramics. J Dent 2000;28:529–35.
[50] Quinn JB, Quinn GD. A practical and systematic review of Weibull statistics for reporting strengths of dental materials. Dent Mater 2010;26:135–47.
[51] Ritter JE. Predicting lifetimes of materials and material structures. Dent Mater 1995;11:142–6.
[52] Nakamura K, Harada A, Ono M, Shibasaki H, Kanno T, Niwano Y, et al. Effect of low-temperature degradation on the mechanical and microstructural properties of tooth-colored 3Y-TZP ceramics. J Mech Behav Biomed Mater 2016;53:301–11.
[53] Ramos GF, Pereira GK, Amaral M, Valandro LF, Bottino MA. Effect of grinding and heat treatment on the mechanical behavior of zirconia ceramic. Braz Oral Res 2016;30.
[54] Tang D, Lim H-B, Lee K-J, Lee K-J, Cho W-S. Evaluation of mechanical reliability of zirconia-toughened alumina composites for dental implants. Ceram Int 2012;38:2429–36.
[55] Nemli SK, Yilmaz H, Aydin C, Bal BT, Tiras T. Effect of fatigue on fracture toughness and phase transformation of Y-TZP ceramics by X-ray diffraction and Raman spectroscopy. J Biomed Mater Res B Appl Biomater 2012;100:416–24.
[56] Denry I, Kelly JR. Emerging ceramic-based materials for dentistry. J Dent Res 2014;93:1235–42.